AIP | Applied Physics Letters

Morphology control of perovskite light-emitting diodes by using amino acid self-assembled monolayers

Nana Wang, Lu Cheng, Junjie Si, Xiaoyong Liang, Yizheng Jin, Jianpu Wang, and Wei Huang

Citation: Applied Physics Letters **108**, 141102 (2016); doi: 10.1063/1.4945330
View online: http://dx.doi.org/10.1063/1.4945330
View Table of Contents: http://scitation.aip.org/content/aip/journal/apl/108/14?ver=pdfcov
Published by the AIP Publishing

Morphology control of perovskite light-emitting diodes by using amino acid self-assembled monolayers

Nana Wang,[1] Lu Cheng,[1] Junjie Si,[2] Xiaoyong Liang,[2] Yizheng Jin,[3] Jianpu Wang,[1,a)] and Wei Huang[1,4]

[1]*Key Laboratory of Flexible Electronics (KLOFE) and Institute of Advanced Materials (IAM), Jiangsu National Synergetic Innovation Center for Advanced Materials (SICAM), Nanjing Tech University (NanjingTech), 30 South Puzhu Road, Nanjing 211816, China*
[2]*State Key Laboratory of Silicon Materials, Center for Chemistry of High-Performance and Novel Materials, and Department of Materials Science and Engineering, Zhejiang University, Hangzhou 310027, China*
[3]*Center for Chemistry of High-Performance and Novel Materials, State Key Laboratory of Silicon Materials, and Department of Chemistry, Zhejiang University, Hangzhou 310027, China*
[4]*Key Laboratory for Organic Electronics and Information Displays and Institute of Advanced Materials (IAM), Jiangsu National Synergetic Innovation Center for Advanced Materials (SICAM), Nanjing University of Posts & Telecommunications, 9 Wenyuan Road, Nanjing 210023, China*

(Received 2 January 2016; accepted 22 March 2016; published online 4 April 2016)

Amino acid self-assembled monolayers are used in the fabrication of light-emitting diodes based on organic-inorganic halide perovskites. The monolayers of amino acids provide modified interfaces by anchoring to the surfaces of ZnO charge-transporting layers using carboxyl groups, leaving the amino groups to facilitate the nucleation of $MAPbBr_3$ perovskite films. This surface-modification strategy, together with chlorobenzene-assisted fast crystallization method, results in good surface coverage and reduced defect density of the perovskite films. These efforts lead to green perovskite light emitting diodes with a low turn-on voltage of 2 V and an external quantum efficiency of 0.43% at a brightness of ~5000 cd m^{-2}. © *2016 AIP Publishing LLC*.
[http://dx.doi.org/10.1063/1.4945330]

Organic-inorganic hybrid perovskites have received significant attention due to their potential applications in low-cost and high-efficiency solar cells.[1–3] Because of the high photoluminescence quantum efficiency, excellent charge mobility, and tunable band-gap, the hybrid perovskites are also promising in light-emitting diode applications.[4–7] After Tan *et al*. first reported effective electroluminescence from three-dimensional perovskite films using a carrier confinement device structure,[5] the performance of perovskite light-emitting diodes (PeLEDs) was significantly improved in the past year and device external quantum efficiency (EQE) as high as over 8% was reported, revealing great potential in low-cost display and lighting fields.[4,8]

Perovskite films with high surface coverage and good emissive properties are the two key issues for achieving high-efficiency PeLEDs,[4,5] and a number of approaches have been introduced to overcome them.[9–11] In perovskite solar cell applications, sequential deposition and two-step spin-coating methods have been widely adopted to get uniform $CH_3NH_3PbI_3$ films.[12,13] However, these methods can lead to reduced grain size and crystallinity of perovskite films, resulting in high defect density and thereby degraded luminance properties.[14,15] Li *et al*. used a blend of perovskite and polyimide precursor dielectric (PIP) to reduce pinholes in perovskite film, which significantly enhanced quantum efficiency of $CH_3NH_3PbBr_3$ PeLEDs. Nevertheless, the obtained luminance of this device is relatively low, due to the presence of the insulator in the emissive layer.[16]

We previously used a multifunctional polyethyleneimine (PEI) interlayer between the oxide electron-transporting layer and the perovskite emissive layer to achieve uniform perovskite thin films with low defect densities.[4] Also, other groups demonstrated that introducing self-assembling monolayers on top of electron-extracting layer was an effective method to enhance the photovoltaic performance of $CH_3NH_3PbI_3$ perovskite solar cells.[17–19] These results suggest that in order to achieve high-quality perovskite films, it is critical to control the surface properties of the underlying layers.

Here, we introduce amino acid monomolecular layers with different alkyl chains (5-ammoniumvaleric acid (5AVA) or 8-aminooctanoic acid (8AOA)) between ZnO and $CH_3NH_3PbBr_3$ film to obtain uniform and low defect density perovskites films. We demonstrate that the amino groups can improve the wetting property of ZnO layers, thereby favoring the growth of perovskite films. We find that $CH_3NH_3PbBr_3$ films with almost full coverage can be achieved on ZnO/5AVA (or 8AOA) substrates with the aid of the chlorobenzene(CB)-induced fast crystallization processes. The morphology and crystallinity improvement lead to significantly enhanced device performance of ZnO-based PeLEDs.

Fig. 1(a) shows the PeLED device structure with multilayers of indium tin oxide (ITO)/amino acid-modified zinc oxide (ZnO, ~20 nm)/$CH_3NH_3PbBr_3$ (~50 nm)/poly(9,9-dioctyl-fluorene-co-N-(4-butylphenyl) diphenylamine) (TFB, ~25 nm)/molybdenum oxide (MoO_x, ~8 nm)/gold (Au, ~100 nm). A schematic of the flat-band energy-level diagram is shown in Fig. 1(b). ITO-coated glass substrates, with an ITO thickness of ~100 nm and a sheet resistance of 15 Ω sq^{-1}, were used for device fabrication. Prior to film deposition, the ITO glass was cleaned thoroughly followed by oxygen plasma treatment.[4]

a)Author to whom correspondence should be addressed. Electronic mail: iamjpwang@njtech.edu.cn

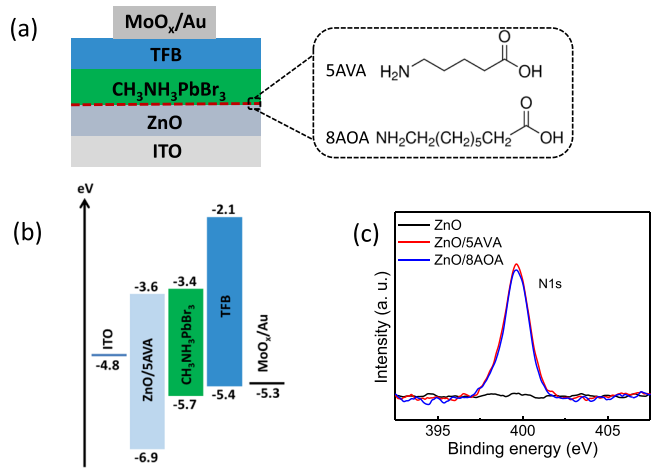

FIG. 1. (a) Schematic illustration of the device configuration of the $CH_3NH_3PbBr_3$ PeLEDs. (b) Flat-band energy level diagram of the $CH_3NH_3PbBr_3$ PeLEDs. (c) XPS spectra (N1s) of the bare ZnO film and 5AVA or 8AOA treated ZnO films.

Then, solutions of ZnO nanocrystals[20] were spin-coated onto the ITO glass substrates at 4000 rpm for 45 s and annealed in air at 150 °C for 30 min (The powder XRD data and film PL spectrum of the ZnO nanocrystals are shown in supplementary Figure S1.[21]). The substrates were immersed in a 1 mg ml^{-1} solution of amino acid (5AVA or 8AOA) in methanol for 1 h to introduce amino acid on the ZnO surface, and rinsed twice by methanol. Then, the substrates were transferred into a glovebox. The $CH_3NH_3PbBr_3$ films were deposited by spin coating the precursor solution (CH_3NH_3Br and $PbBr_2$ with 3:1 molar ratio in N,N-dimethylformamide (DMF)) onto the amino acid treated ZnO films, followed by annealing on a hot plate at 60 °C. Alternatively, the substrates were treated by drop-casting CB during spin-coating $CH_3NH_3PbBr_3$ precursor. The TFB layers were deposited from an m-xylene solution (8 mg ml^{-1}) at 2000 rpm. Finally, the MoO_x/Au electrodes were sequentially thermally evaporated at a rate of 0.05 nm s^{-1} through a shadow mask under a base pressure of $\sim 6 \times 10^{-7}$ Torr. The device area was 3.24 mm^2 as defined by the overlapping area of the ITO films and top electrodes.

All PeLEDs were encapsulated with glass lid using UV-resin in a high-purity N_2-filled glovebox. A Keithley 2400 source meter and a fiber integration sphere (FOIS-1) couple with a QE-6500 spectrometer were used for the measurements.[22,23] A field emission scanning electron microscope (SEM) (SU-70) was used to obtain SEM images. X-ray photoelectron spectroscopy (XPS) spectra were collected on a Thermo ESCALAB 250 equipment in an ultrahigh vacuum chamber with a vacuum of $<10^{-10}$ Torr. Photoluminescence (PL) spectra of the perovskite films and the time resolved fluorescence spectra were obtained using an Edinburgh Instruments (FLS920) spectrometer. For the time-resolved PL measurements, the perovskite films were excited by a 405 nm pulsed diode laser (EPL-405) with a fluence of $\sim$4 nJ cm^{-2}.

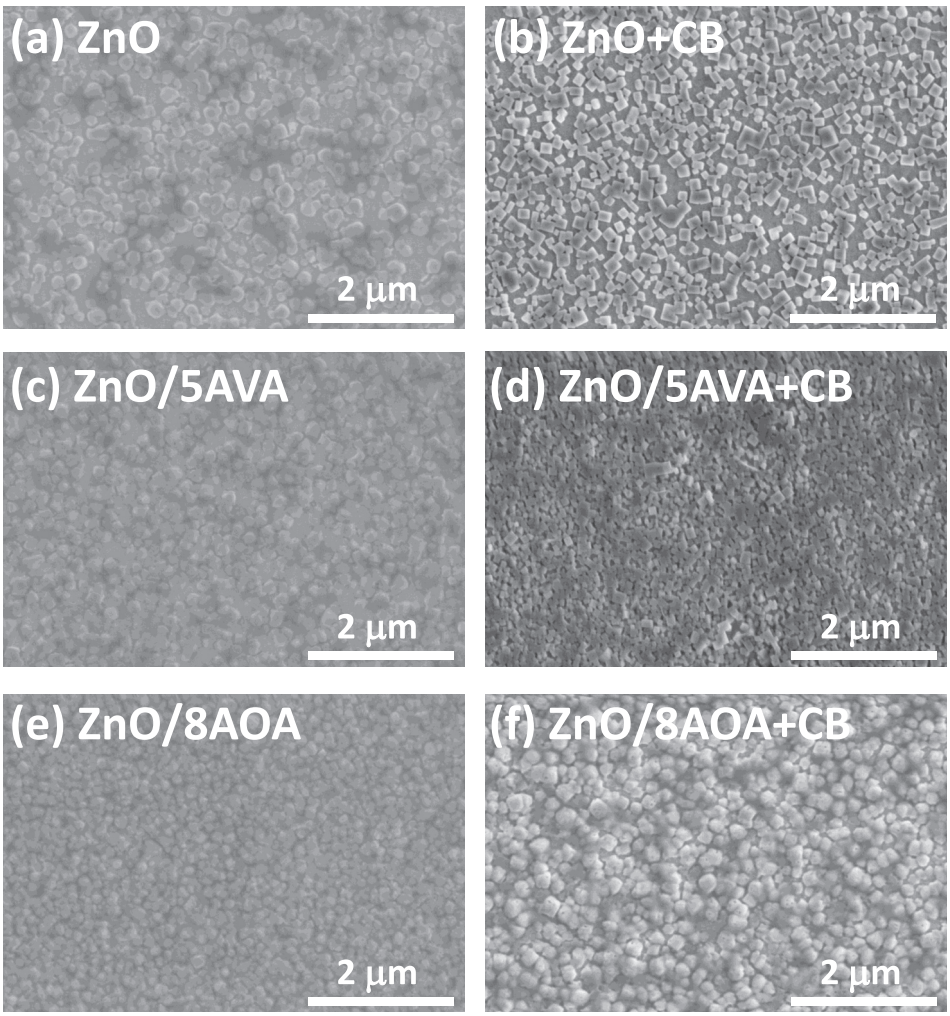

FIG. 2. SEM images of $CH_3NH_3PbBr_3$ films on (a) and (b) bare ZnO. (c) and (d) ZnO/5AVA. (e) and (f) ZnO/8AOA. (a), (c), and (e) represent $CH_3NH_3PbBr_3$ films prepared by conventional spin-coating process and (b), (d), and (f) show $CH_3NH_3PbBr_3$ films prepared by solvent engineering method. The coverage of $CH_3NH_3PbBr_3$ films in (a)–(f) (estimated from SEM images by ImageJ Software) are 63%, 68%, 77%, 92%, 85%, and 89%, respectively.

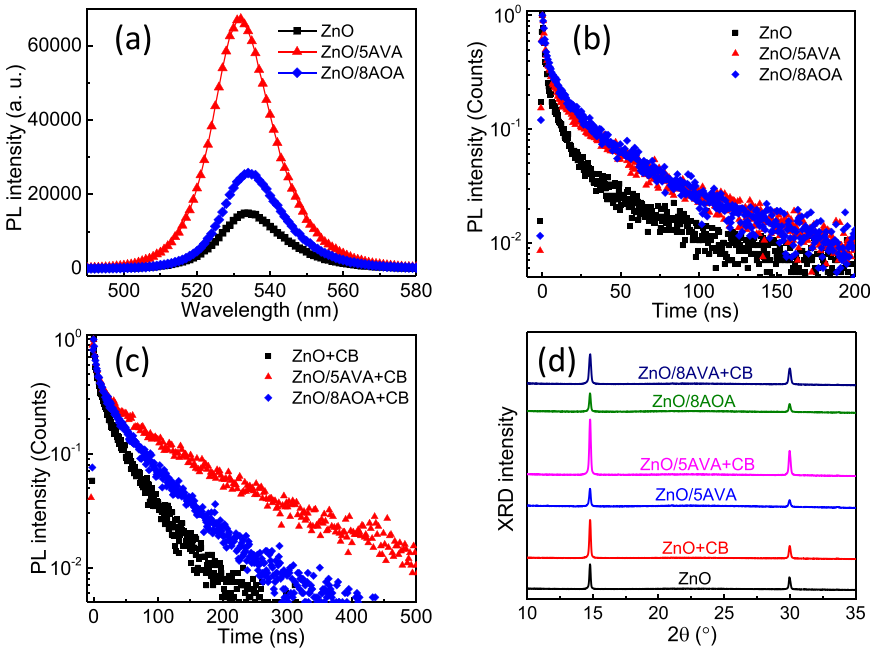

FIG. 3. (a) PL spectra of $CH_3NH_3PbBr_3$ film formed on top of the ZnO, ZnO/5AVA, ZnO/8AOA layers. (b) Time-resolved PL decay transient showing the PL lifetime for the $CH_3NH_3PbBr_3$ formed on top of the ZnO, ZnO/5AVA, and ZnO/8AOA layers, respectively. (c) Time-resolved PL decay transient showing the PL lifetime for the $CH_3NH_3PbBr_3$ formed on different substrates by solvent engineering. (d) XRD data of the $CH_3NH_3PbBr_3$ films on different substrates.

The assembly of amino acid onto the ZnO surface can be realized by the formation of covalent bonds between the carboxyl groups and Zn ions.[17,24] In order to verify this surface modification process, the surface composition was characterized with XPS as shown in Figure 1(c). The peaks at 400 eV represent the binding energy of N1s related to NH_2,[25] indicating the modification of amino acid on ZnO. However, due to the residual zinc acetate in ZnO film, it is difficult to directly show the presence of the C=O or C–O groups.

SEM images of $CH_3NH_3PbBr_3$ films on ZnO with different SAM layers are shown in Fig. 2. The formation and coverage of $CH_3NH_3PbBr_3$ film were extremely poor on bare ZnO films.[4] After introducing 5AVA or 8AOA between ZnO and $CH_3NH_3PbBr_3$ film, the film coverage of $CH_3NH_3PbBr_3$ is significantly improved. The improved morphology is probably due to hydrogen-bonding or electrostatic interactions between the amino groups and the perovskites framework,[26] which can facilitate the nucleation of $CH_3NH_3PbBr_3$ crystals.

Figures 3(a) and 3(b) show the PL spectra and PL decay of $CH_3NH_3PbBr_3$ films on different substrates. It can be seen that the PL spectra of $CH_3NH_3PbBr_3$ are consistent with different substrates, while the PL intensity on amino acid modified ZnO was significantly increased, especially on 5AVA SAM. Moreover, the PL lifetime (1/e of the initial value) for the $CH_3NH_3PbBr_3$ film was increased to ~4 ns after the modification of 5AVA or 8AOA monolayer (Figure 3(b)). The increased PL lifetime is consistent with the morphology improvement as shown in Fig. 2, which may be due to lower defect densities in the perovskite bulk films or reduced surface defects.

Fig. 4(a) shows the electroluminescence (EL) emission peaked at 536 nm, which is consistent with the PL emission

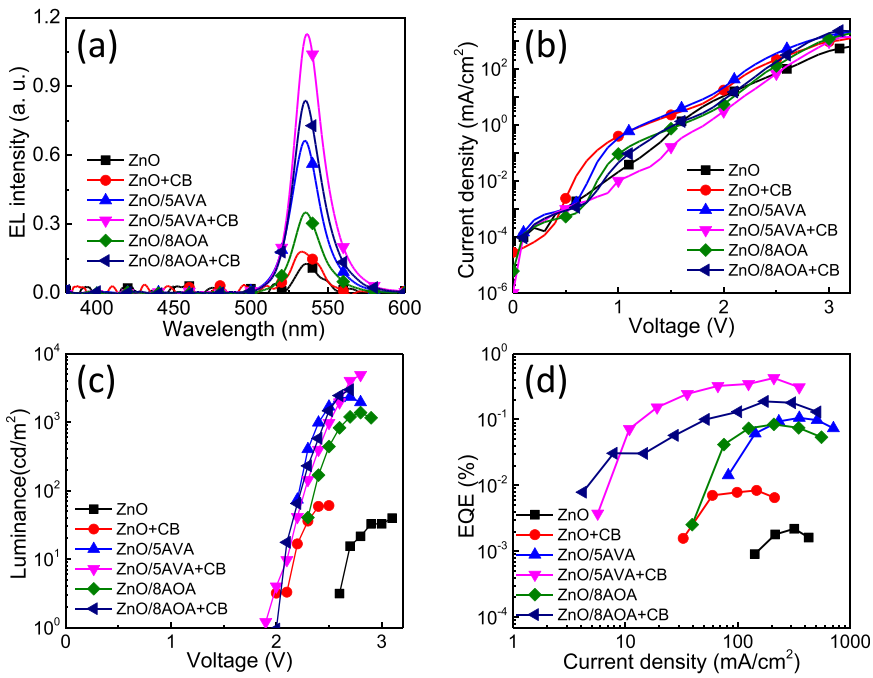

FIG. 4. Optoelectronic characteristics of the $CH_3NH_3PbBr_3$ PeLEDs. (a) Electroluminescence spectra of the device under bias (ZnO, 3.2 V, ZnO + CB, 2.5 V, others, 2.7 V). (b) Dependence of current density on the driving voltage. (c) Dependence of luminance on the driving voltage. (d) EQE versus current density.

TABLE I. Performance of PeLEDs with different interfacial layers and film formation processes. We measured over 20 devices for each structure and the relative standard deviations in peak EQEs are below 15%.

Device	V_{on} (V)	$Luminance_{max}$ (cd m^{-2})	EQE_{max} (%)
ZnO	2.6	40	0.002
ZnO/5AVA	2.2	2330	0.11
ZnO/8AOA	2.3	1370	0.08
ZnO + CB	2	60	0.008
ZnO/5AVA + CB	1.9	4890	0.43
ZnO/8AOA + CB	2	2970	0.19

spectrum of the $CH_3NH_3PbBr_3$ perovskite film. No electroluminescence from the ZnO or TFB layers can be detected. The device parameters of PeLEDs with or without SAM are compared in Fig. 4 and Table I. The device on bare ZnO substrate has a turn-on voltage of 2.6 V and a maximum luminance of 40 cd m^{-2} at 3.2 V. After introducing SAM, the device with ZnO/5AVA layer has a reduced turn-on voltage of 2.2 V, where an EQE of 0.11% is achieved at a luminance of 2000 cd m^{-2}. Similar enhancement is observed for devices fabricated on 8AOA modified ZnO films, showing that amino acid SAM can effectively improve the PeLEDs device performance by tuning the interfacial properties. Apart from the high crystallinity and uniform surface of $CH_3NH_3PbBr_3$ films using the SAMs, the increase in device performance could also be from the reduction of energy barrier between ZnO and $CH_3NH_3PbBr_3$ emitter.[4] To determine whether the SAMs have effects on changes in energy barrier, we measured the work function of ZnO with or without SAM using ultraviolet photoelectron spectroscopy (UPS). The UPS data show that the work function of ZnO, ZnO/5AVA, ZnO/8AOA are 3.6 eV, 3.6 eV, and 3.5 eV, respectively. This minor variation of ZnO work function is unlikely to contribute to the significant enhancement of the PeLED device performance.

Based on the above analyses, we suggest that the improvements of the morphology of the perovskite films can effectively enhance the PeLED device performance. However, as shown in Figs. 2(c) and 2(e), some pin-holes still exist in the $CH_3NH_3PbBr_3$ films on SAM modified ZnO layer. In order to further improve the film uniformity, we use chlorobenzene to assist crystallization of $CH_3NH_3PbBr_3$.[27,28] As shown in Figs. 2(b), 2(d), and 2(f), the solvent engineering method can significantly improve the morphology of perovskite films on top of SAM modified ZnO layer. $CH_3NH_3PbBr_3$ films with almost full coverage can be realized using the 5AVA SAM modification combining with the quick crystallization process. After using CB-assisted film formation method, the PL lifetimes of the $CH_3NH_3PbBr_3$ films were also increased, from ~4 ns to ~14 ns (Fig. 3(c)), indicating reduced defects. As shown in Fig. 3(d), the X-ray diffraction data show that all $CH_3NH_3PbBr_3$ diffraction peaks were enhanced after increasing crystallization rate, especially for films on 5AVA SAM. The full-width-at-half-maximum of their diffraction peaks almost remains the same, suggesting that in our experiment, the CB-assisted film formation method does not increase the grain size, while mainly improves the surface coverage of the perovskite films.

PeLED devices are also fabricated based on the obtained more uniform and less defect perovskite films using solvent engineering method as shown in the Fig. 4. The device on ZnO exhibits a decreased turn-on voltage of 2 V and an increased EQE of 0.01%. However, the EQE is still low due to the discontinuous $CH_3NH_3PbBr_3$ film. Furthermore, the device on ZnO/5AVA layer achieves a maximum EQE of 0.43% at 2.7 V and a maximum luminance of ~5000 cd m^{-2}, corresponding to a 200 times increase to that of control device without interface modification and solvent treatment of perovskite film. The CB solvent method also worked for perovskite film on 8AOA modified ZnO, showing a maximum EQE of 0.19% at 2.7 V and a luminance of 2970 cd m^{-2}. The fact that the 5AVA devices show superior performance than 8AOA devices indicates the importance of appropriate chain length in assistance of perovskite film formation. We note that similar effect has been observed previously in perovskite solar cells.[2]

In conclusion, we have demonstrated that the amino-acid SAMs are effective in tuning the interfacial properties of ZnO/perovskite, thereby improving PeLEDs performance by increasing film quality of the $CH_3NH_3PbBr_3$ emitter. The amino group assembled on ZnO by carboxy group can facilitate the nucleation and growth of $CH_3NH_3PbBr_3$ perovskites with increasing film coverage and reducing defect states. Using chlorobenzene-induced fast crystallization method, the film crystallization and morphology can be further improved on top of the SAM modified ZnO layers, leading to significantly (~200 times) improved PeLED device performance.

This work was financially supported by the Fundamental Studies of Perovskite Solar Cells (2015CB932200), Jiangsu Natural Science Foundation (BK20131413 and BK20140952), Jiangsu Specially-Appointed Professor program, National Natural Science Foundation of China (51172203, 61405091, and 11474164), China Postdoctoral Science Foundation, and the Synergetic Innovation Center for Organic Electronics and Information Displays. We thank Professor Haiping He and Miss Qianqian Yu (Zhejiang University) for the assistance of TCSPC measurements. We thank Professor Hongwei Han (Huazhong University of Science and Technology) for useful discussions.

[1]H. Zhou, Q. Chen, G. Li, S. Luo, T. Song, H.-S. Duan, Z. Hong, J. You, Y. Liu, and Y. Yang, Science **345**, 542 (2014).
[2]A. Mei, X. Li, L. Liu, Z. Ku, T. Liu, Y. Rong, M. Xu, M. Hu, J. Chen, Y. Yang, M. Grätzel, and H. Han, Science **345**, 295 (2014).
[3]N. J. Jeon, J. H. Noh, W. S. Yang, Y. C. Kim, S. Ryu, J. Seo, and S. I. Seok, Nature **517**, 476 (2015).
[4]J. Wang, N. Wang, Y. Jin, J. Si, Z.-K. Tan, H. Du, L. Cheng, X. Dai, S. Bai, H. He, Z. Ye, M. L. Lai, R. H. Friend, and W. Huang, Adv. Mater. **27**, 2311 (2015).
[5]Z.-K. Tan, R. S. Moghaddam, M. L. Lai, P. Docampo, R. Higler, F. Deschler, M. Price, A. Sadhanala, L. M. Pazos, D. Credgington, F. Hanusch, T. Bein, H. J. Snaith, and R. H. Friend, Nat. Nanotechnol. **9**, 687 (2014).
[6]Y.-H. Kim, H. Cho, J. H. Heo, T.-S. Kim, N. Myoung, C.-L. Lee, S. H. Im, and T.-W. Lee, Adv. Mater. **27**, 1248 (2015).
[7]N. Wang, J. Si, Y. Jin, J. Wang, and W. Huang, Acta Chimica Sinica **73**, 171 (2015).

[8]H. Cho, S.-H. Jeong, M.-H. Park, Y.-H. Kim, C. Wolf, C.-L. Lee, J. H. Heo, A. Sadhanala, N. Myoung, S. Yoo, S. H. Im, R. H. Friend, and T.-W. Lee, Science **350**, 1222 (2015).
[9]R. L. Z. Hoye, M. R. Chua, K. P. Musselman, G. Li, M.-L. Lai, Z.-K. Tan, N. C. Greenham, J. L. MacManus-Driscoll, R. H. Friend, and D. Credgington, Adv. Mater. **27**, 1414 (2015).
[10]O. A. Jaramillo-Quintero, R. S. Sanchez, M. Rincon, and I. Mora-Sero, J. Phys. Chem. Lett. **6**, 1883 (2015).
[11]N. K. Kumawat, A. Dey, A. Kumar, S. P. Gopinathan, K. L. Narasimhan, and D. Kabra, ACS Appl. Mater. Interfaces **7**, 13119 (2015).
[12]J. Burschka, N. Pellet, S.-J. Moon, R. Humphry-Baker, P. Gao, M. K. Nazeeruddin, and M. Grätzel, Nature **499**, 316 (2013).
[13]Z. Xiao, C. Bi, Y. Shao, Q. Dong, Q. Wang, Y. Yuan, C. Wang, Y. Gao, and J. Huang, Energy Environ. Sci. **7**, 2619 (2014).
[14]V. D'Innocenzo, A. R. Srimath Kandada, M. De Bastiani, M. Gandini, and A. Petrozza, J. Am. Chem. Soc. **136**, 17730 (2014).
[15]Y. Yang, Y. Yan, M. Yang, S. Choi, K. Zhu, J. M. Luther, and M. C. Beard, Nat. Commun. **6**, 7961 (2015).
[16]G. Li, Z.-K. Tan, D. Di, M. L. Lai, L. Jiang, J. H. Lim, R. H. Friend, and N. C. Greenham, Nano Lett. **15**, 2640 (2015).
[17]L. Zuo, Z. Gu, T. Ye, W. Fu, G. Wu, H. Li, and H. Chen, J. Am. Chem. Soc. **137**, 2674 (2015).
[18]L. Liu, A. Mei, T. Liu, P. Jiang, Y. Sheng, L. Zhang, and H. Han, J. Am. Chem. Soc. **137**, 1790 (2015).
[19]J. C. Yu, D. B. Kim, G. Baek, B. R. Lee, E. D. Jung, S. Lee, J. H. Chu, D.-K. Lee, K. J. Choi, S. Cho, and M. H. Song, Adv. Mater. **27**, 3492 (2015).
[20]L. Qian, Y. Zheng, K. R. Choudhury, D. Bera, F. So, J. Xue, and P. H. Holloway, Nano Today **5**, 384 (2010).
[21]See supplementary material at http://dx.doi.org/10.1063/1.4945330 for detail of the ZnO nanocrystals.
[22]X. Dai, Z. Zhang, Y. Jin, Y. Niu, H. Cao, X. Liang, L. Chen, J. Wang, and X. Peng, Nature **515**, 96 (2014).
[23]S. Bai, M. Cao, Y. Jin, X. Dai, X. Liang, Z. Ye, M. Li, J. Cheng, X. Xiao, Z. Wu, Z. Xia, B. Sun, E. Wang, Y. Mo, F. Gao, and F. Zhang, Adv. Energy Mater. **4**, 1301460 (2014).
[24]E. Tang, G. Cheng, and X. Ma, Powder Technol. **161**, 209 (2006).
[25]A. P. Dementjev, A. de Graaf, M. C. M. van de Sanden, K. I. Maslakov, A. V. Naumkin, and A. A. Serov, Diamond Related Mater. **9**, 1904 (2000).
[26]S. Zhang, P. Audebert, Y. Wei, A. Al Choueiry, G. Lanty, A. Bréhier, L. Galmiche, G. Clavier, C. Boissière, J.-S. Lauret, and E. Deleporte, Materials **3**, 3385 (2010).
[27]N. J. Jeon, J. H. Noh, Y. C. Kim, W. S. Yang, S. Ryu, and S. I. Seok, Nat. Mater. **13**, 897 (2014).
[28]M. Xiao, F. Huang, W. Huang, Y. Dkhissi, Y. Zhu, J. Etheridge, A. Gray-Weale, U. Bach, Y.-B. Cheng, and L. Spiccia, Angew. Chem. **126**, 10056 (2014).